J. Am. Soc. Mass Spectrom. (2016) 27:1301–1313
DOI: 10.1007/s13361-016-1400-6

RESEARCH ARTICLE

# Negative Ion MALDI Mass Spectrometry of Polyoxometalates (POMs): Mechanism of Singly Charged Anion Formation and Chemical Properties Evaluation

Jean E. Boulicault, Sandra Alves, Richard B. Cole

Sorbonne Universités, UPMC Univ Paris 06, CNRS, Institut Parisien de Chimie Moléculaire (IPCM), 4 place Jussieu, 75252, Paris Cedex 05, France

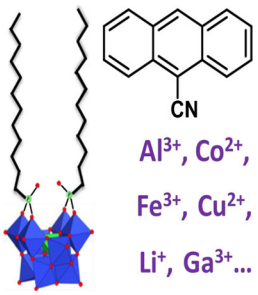


**Abstract.** MALDI-MS has been developed for the negative ion mode analysis of polyoxometalates (POMs). Matrix optimization was performed using a variety of matrix compounds. A first group of matrixes offers MALDI mass spectra containing abundant intact singly charged anionic adduct ions, as well as abundant in-source fragmentations at elevated laser powers. A relative ranking of the ability to induce POM fragmentation is found to be: DAN > CHCA > CNA > DIT> HABA > DCTB > IAA. Matrixes of a second group provide poorer quality MALDI mass spectra without observable fragments. Sample preparation, including the testing of salt additives, was performed to optimize signals for a model POM, POMc12, the core structure of which bears four negative charges. The matrix 9-cyanoanthracene (CNA) provided the best signals corresponding to singly charged intact POMc12 anions. Decompositions of these intact anionic species were examined in detail, and it was concluded that hydrogen radical-induced mechanisms were not prevalent, but rather that the observed prompt fragments originate from transferred energy derived from initial electronic excitation of the CNA matrix. Moreover, in obtained MALDI mass spectra, clear evidence of electron transfer to analyte POM species was found: a manifestation of the POMs ability to readily capture electrons. The affinity of polyanionic POMc12 toward a variety of cations was evaluated and the following affinity ranking was established: $Fe^{3+} > Al^{3+} > Li^{+} > Ga^{3+} > Co^{2+} > Cr^{3+} > Cu^{2+} > [Mn^{2+}, Mg^{2+}] > [Na^{+}, K^{+}]$. Thus, from the available cationic species, specific adducts are preferentially formed, and evidence is given that these higher affinity POM complexes are formed in the gas phase during the early stages of plume expansion.

**Keywords:** Negative Ion MALDI, Polyoxometalates (POMs), In-source decay, MALDI mechanisms, Cationic adduct, Fragmentation

Received: 8 November 2015/Revised: 29 March 2016/Accepted: 30 March 2016/Published Online: 3 May 2016

## Introduction

Since the late 1980s, matrix-assisted laser desorption ionization (MALDI) has become a major ionization technique for mass spectrometric studies, especially regarding large molecule analysis that one encounters in the proteomics and polymer fields. Upon closer examination, the use of MALDI can be found in a rather wide variety of applications, including glycans analysis [1] and, more generally, for investigations of all types of large biomolecules [2]. The small sample quantity required to perform an analysis has earned the MALDI technique renown as an exceptionally sensitive tool that is more tolerant of the presence of salts than other mass spectrometric ionization techniques (e.g., electrospray ionization). In addition, the possibility for label-free detection of a wide array of molecules, and the application of focused lasers for desorption/ionization at rather high spatial resolution, have attracted increasing attention for imaging mass spectrometry analysis [3]. However, the major bottleneck of MALDI applications is the sample preparation step that initially involves finding an efficient matrix, and subsequently involves optimization of target preparation. Sample preparation is still largely performed empirically, even if many recipes are known and have undergone amelioration over time [4].

Even though much effort has been invested in increasing knowledge concerning details of MALDI processes, the comprehension of the exact mechanisms of the involved desorption/

**Electronic supplementary material** The online version of this article (doi:10.1007/s13361-016-1400-6) contains supplementary material, which is available to authorized users.

*Correspondence to:* Richard B. Cole; *e-mail:* richard.cole@upmc.fr

ionization is still on-going. Some models portray the MALDI process as commencing with the formation of huge aggregates of matrix [5] where analytes can be either precharged ("Lucky Survivor" model) [6], or can interact with charged matrix molecules to finish as naked intact protonated (or deprotonated for negative mode) species [7]. Mechanistic studies concerning the ionization process are typically undertaken in the positive ion mode, and they mainly consider proton and/or electron transfers as being responsible for analyte charging.

Despite the fact that MALDI is much more used in the positive ion mode, it also seems important to develop studies in the negative ion mode that may improve the fundamental understanding of the ion formation process. The negative ion mode has been less frequently employed, with the exception of its application toward specific compound classes, such as DNA [8] , sugars [1], and lipids [9].

To widen the array of applications using negative mode MALDI analysis, we present results pertaining to polyoxoanionic species, [i.e., polyoxometalates (POMs)]. These polyanionic species are early-transition metal-oxygen structures that can be functionalized by organic and/or inorganic groups, thereby allowing the "tuning" of POM properties such as redox behavior, magnetic and acid-base characteristics, or even biocompatibility [10]. The large variability of POM structures has resulted in a wide range of different properties and a corresponding range of potential chemical and biological applications. For example, POMs have found industrial applications for organic compound oxidation or dehydration [11], and they are promising tools for photovoltaic applications [12].

Functionalized polyoxometalate anions commonly have a charge state varying between 2 and 12 [10] and the tendency has been to perform mass spectrometric analyses using electrospray ionization (ESI). The obtained mass spectra typically display several charge states corresponding to various adducted forms of intact molecular ions. Analysis of POMs by MALDI is a challenge because of the numerous charges that the POMs possess, but singly charged ions have been observed for small molecules [3]. MALDI and LDI analyses were reported for characterization of unfunctionalized POM cores in negative ion mode [13, 14], and polymers containing POM structures were even characterized in positive ion mode [15, 16]. However, to our knowledge, no fragile polyoxoanionic structures containing functionalization have been reported as intact molecular species using MALDI or LDI in the negative ion mode. A study concerning polyanionic dendrimer species has been published but despite the presence of multiple negative anionic substituents the molecules remain in salt form with cations associated with each negative moiety, plus one additional cation to render the dendrimers detectable as singly charged intact cations [17].

This article reports on MALDI investigations of functionalized POMs, with special focus placed upon a model POM, denoted POMc12, the ionization behavior of which was characterized in the presence of various matrixes and using different means of target preparation (e.g., salt addition). The effect of matrix choice and sample preparation on mass spectrum quality has undergone a detailed evaluation. Among the tested matrixes, 9-cyanoanthracene, which is a rather unusual matrix, even if its use was reported once by Limbach and Robins as a suitable matrix for crude oil analysis [18], proved its capability to readily desorb and ionize the model POM. The energetic behavior of this matrix, through the ability to both allow molecular ion detection and induce specific in-source fragmentations, was compared with other matrixes. These comparisons led to a general matrix classification according to the ability to induce in-source dissociations. The competition between cations to either produce an intact adduct ion or to produce cation-containing fragments was studied to establish a ranking of cationic attachment preferences.

## Experimental

### *Materials*

*Matrixes* The standard matrixes, α-cyano-4-hydroxycinnamic acid (CHCA), sinapic acid (SA), 3-hydroxypicolinic acid (HPA), 2′,4′,6′-trihydroxyacetophenone (THAP), trans-3-indoleacrylic acid (IAA), 2-(4-hydroxyphenylazo)benzoic acid (HABA), dithranol, 1,5-diaminonaphtalene (DAN), 2-[(2E)-3-(4-tert-butylphenyl)-2-methylprop-2-enylidene]malononitrile (DCTB) were purchased from Sigma-Aldrich (St. Quentin Fallavier, France) as high-purity MALDI matrix grade and were used without further purification. Aqueous solutions of salt additives (LiCl, NaCl, KCl, $MgCl_2(6H_2O)$, $CuSO_4(5H_2O)$, $CoCl_2(6H_2O)$, $AlCl_3$, $CrCl_3$, $FeCl_3(6H_2O)$, $Fe(NO_3)_3(9H_2O)$, $GaCl_3$, and $Fe(NO_3)_3$ were prepared with a cation concentration of 0.5 M in deionized MilliQ water (Millipore, Darmstadt, Germany). The 9-anthracenecarbonitrile (CNA) 97% (CAS 1210-12-4) matrix was purchased from Sigma-Aldrich and purified by solubilization and precipitation with mixtures of deionized water and HPLC grade tetrahydrofuran (THF) or acetonitrile ($CH_3CN$) in different proportions. The precipitate obtained underwent a final wash using HPLC grade ethanol and was left to dry at room temperature. Upon recrystallization, the powder, initially colored yellow-khaki, became yellow.

*Polyoxometalates* The polyoxometalates used throughout this study were synthesized at the IPCM [19] and were graciously donated for this study. POMc12 is built with 10 tungsten-oxides distributed around a central silicate nucleus, grafted with two linear alkylphosphonium chains. This quadruply negatively charged compound with original formula $TMA_3K[SiW_{10}O_{36}(POC_{12}H_{25})_2]$ was weighed in its salt form and was directly solubilized in acetonitrile at 1 g/L.

### *Sample Preparation for MALDI Analyses*

Two kinds of MALDI plates were used in our analyses. The first is a stainless steel plate; the second is a polymer plate, prespotted with CHCA spots jointly developed by Bruker and

Eppendorf (Bruker Daltonics, Inc., Bremen, Germany). The polymer plate of 1.25 mm thickness was cleaned with a similar procedure as was applied to the stainless steel plates. Washes were performed with a mix of deionized water and acetonitrile (~400 mL) followed successively by washes with acetic acid and then sodium hydroxide (1 M solutions). Afterwards, a wash with cyclohexane followed by ethanol was performed to remove hydrophobic compounds. A final $CH_3CN$ wash left the plate clean and dry.

In order to minimize any differences in behavior due to solubility differences for the various matrixes, a special ternary solvent capable of solubilizing all the used matrices at a concentration of 10 g/L was employed. This solvent is composed of $CH_3CN$-THF-water in a 5/4/1 (v/v/v) volumic proportion. This solvent mixture ensured that all tested matrixes were soluble and that introduced salt remained soluble. All the matrixes were dissolved and vortexed at 10 g/L without any acidification. Aqueous salt solutions were introduced in matrix solution in order to obtain matrixes with 5 mM cation concentrations using the following salts: LiCl, NaCl, KCl, $MgCl_2(6H_2O)$, $CuSO_4(5H_2O)$, $CoCl_2(6H_2O)$, $AlCl_3$, $CrCl_3$, $FeCl_3(6H_2O)$, $Fe(NO_3)_3(9H_2O)$, and $GaCl_3$. Mixtures prepared initially with $FeCl_3$ showed unexpected adduct species that presumably contained chloride, so the nitrate equivalent was used instead, and no further counter-ions were observed or studied, even though counter-ions have previously shown some influence on MALDI results [20]. Moreover, salt precipitation was observed with iron(III) nitrate when matrix solution was prepared in advance, so matrix solutions were prepared just prior to analyses and were deposited on the MALDI plate, along with analytes, without delay. For the cation competition study, solutions containing two salts were obtained by mixing two previously prepared matrix solutions, ending in CNA matrix solutions containing 2.5 mM concentrations of each salt.

Analytes and matrixes were mixed and spotted using the dried droplet method [21]. A 1 μL drop of matrix was spotted on the plate; each deposition was repeated two times for qualitative studies, or three times when peak intensities had to be considered for fragmentation yield calculations.

### *Mass Spectrometry*

MALDI-TOF MS experiments were performed on an Autoflex III instrument (Bruker Daltonics, Inc., Bremen, Germany), equipped with a SmartBeam Nd:YAG laser emitting at 355 nm. Typically, 200 laser shots were accumulated to obtain a mass spectrum; each shot had a duration of 3 ns and a spot size diameter of approximately 50 μm. The repetition rate was 20 Hz. An extraction delay of 80 ns was used when employing detection in the reflectron mode, and ions under *m/z* 850 were not recorded in either ion mode, so as to preserve detectors. For high mass calibration (i.e., *m/z* 900 to *m/z* 3500), a calibration mix comprised of six peptides in a CHCA matrix was employed. The mass error for an obtained calibration curve was less than 10 ppm.

The employed laser power value can be attenuated by use of an adjustable diaphragm, and it can be varied downward from a maximum value of 100 μJ. In order to compare the fragmentation yields obtained for various spot preparation methods, the laser power is expressed in comparison with the specific matrix's threshold laser power. Typically, a laser power of approximately 1.5 times the laser threshold value was used for each matrix to obtain in-source decay (ISD). No other parameters were modified because the optimum delay time observed for ISD fragments seems to be in agreement with standard MALDI-TOF/MS experiments [22].

MS/MS experiments using LIFT mode (Bruker Daltonics) were performed using Argon as collision gas (pressure about $10^{-6}$ mBar). Alternatively, MALDI-TOF/TOF tandem mass spectra were acquired using the Applied Biosystems 4700 Proteomics Analyzer (ABSciex, Concord, Ontario, CA). MALDI-TOF mass spectra of the samples were acquired in reflector mode using delayed extraction and a focus mass set at 2100 u, with a laser power just above the threshold for desorption/ionization and the low mass cut-off set at *m/z* 1000. MALDI-TOF/TOF fragmentation experiments were carried out either without addition of collision gas (residual pressure $2 \times 10^{-8}$ Torr, favoring metastable decompositions), or under CID conditions ($N_2$ at $2 \times 10^{-7}$ Torr, with a collision energy of 1 keV).

## Results and Discussion

A variety of polyoxometalates (POMs), including POMc12, were subjected to MALDI-TOF experiments. MALDI mass spectra were recorded from *m/z* 900–3500, and each prepared sample was tested in both positive and negative ion modes. Above *m/z* 3500, no identifiable signals were observed, whereas below *m/z* 900, ion matrix interferences combined with abundant low mass fragments could saturate the detector in both +/– polarity modes. The molecular mass of POMc12, without counter-ions is 2875 Da (form with four negative charges) and the monoisotopic peak is centered in the middle of the wide isotopic pattern. This hybrid compound, combining organic and inorganic structures, acts as a catalytic reagent to oxidize alkenes in microemulsions. It is able to sequester electrons provided by hydrogen peroxide, and subsequently deliver them to epoxy compounds [19]. With the exception of one instance where a mixture of POMc12 and $Li^+$ produced an ion corresponding to $[POMc12 + 5Li]^+$, no other combination of POM/salt allowed the detection of intact POM signals in the positive ion mode. The results that follow all pertain to the negative ion mode and, unexpectedly, all the signals observed revealed singly charged species, despite the inherent polyanionic nature of POMs. Moreover, the numerous isotopes of tungsten, combined with the fact that each analyte contains 10 tungsten atoms, invariably produced a wide isotopic pattern for each species present. The readily visible nature of this isotopic pattern, characteristic of each POM, presents an advantage for identifying POM species. However, it also

introduces a drawback in the case of ions having close *m/z* values because of the overlap of the respective isotopic patterns. When extensive superposition of isotope patterns occurs, there is a difficulty to unequivocally attribute a unique formula to each peak.

## *Method Development for POMs Analysis in Negative Ion MALDI MS*

The development of MALDI-TOF methods targeting the analysis of negatively charged compounds such as the polyanionic POMs has lagged behind method development in the positive ion mode. In order to commence this study, many commonly used matrixes (CHCA, DHB, IAA, HABA, HPA, SA, THAP, FA, DIT, DCTB) were systematically tested to gauge their desorption/ionization ability. Because of the polyoxometalates' capability to store electrons, many anthracene compounds, known to interact and transfer electrons during MALDI processes [23], were also tried as matrixes. The matrixes CNA, dithranol, and DCTB allow the production of abundant signals above the molecular weight of the "naked" POMs (i.e., 4– charged POM). The best results in terms of peak abundances and signal profiles (corresponding most closely to the theoretical isotopic distribution) were obtained with the CNA matrix (Figure 1). Owing to the labile functionalization present on our compounds, we also investigated the use of surfactants as MALDI additives; such additives have shown the ability to assist in the generation of abundant protonated molecules for MALDI analysis of labile-acid peptides [24]. Sodium dodecyl sulfate induced a notable improvement, but apparently it was not due to surfactant properties. Rather, it was the introduced sodium cation, which helped to promote intact analyte desorption/ionization. The result was that the signal intensity in the region of the POMc12 molecular ion became somewhat improved owing especially to the emergence of singly charged anions containing sodium and other cations such as protons or potassium (see Supplementary Materials, Figure S1). The use of sodium chloride introduced into matrix solutions led to MALDI mass spectra displaying similar singly charged adduct species incorporating sodium and/or other cations. Thus, numerous intact species were produced whose isotopic clusters are overlapping, thereby complicating peak assignments. Nonetheless, this experimental observation confirms that addition of cationic salts tends to improve POMc12 MALDI desorption/ionization.

Upon achieving success with singly charged cations, and bearing in mind that there are four negative charges held by the analyte, a wide range of cations with different charge states were tested. The separate use of many different cations permits the observation of molecular singly charged adduct species, (e.g., $[POMc12 + 3Li]^-$, $[POMc12 + Ga]^-$, or $[POMc12 + Al]^-$, see Figure 1). However, as often occurs in MALDI analysis, no multiply charged species were detected [25], regardless of the employed instrumental parameters and target preparation used (including the presence of additives).

Signals obtained using the CNA matrix without salt addition led to the production of a weak signal at *m/z* 2860, which is assigned as a singly charged fragment ion $[POMc12\text{-}O + H]^-$, and numerous other overlapping signals (as evidenced by the extended isotope patterns observed) at higher *m/z* values (data not shown). These unresolved signals that are clearly constituted of tungsten cores could be considered to represent adducts of POMc12 that incorporate various cations that are present in the bulk. Note that POMc12 is initially synthesized with potassium and trimethylammonium (TMA) counter-ions. Routine ESI-MS analysis performed in our laboratory [19] revealed the presence of these cations in adduct species of intact POMs. Surprisingly, MALDI analysis in the negative ion mode never showed molecular adduct ions containing TMA as counter-ions. This result contrasts with what was observed for a different POM structure in positive ion mode by Mayer et al. [15]. Using the CNA matrix doped with

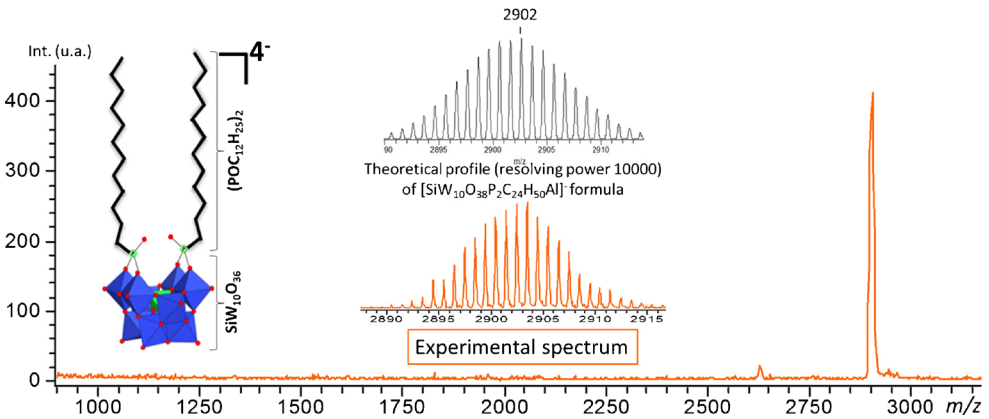


**Figure 1.** Experimental negative ion MALDI mass spectrum of POMc12 in CNA matrix with added $AlCl_3$ acquired at just above laser power threshold with 200 laser shots (orange traces, bottom middle showing region of molecular ion $[POMc12 + Al]^-$, and bottom showing full spectrum); (inset left) representation of POMc12 structure (blue octahedrons correspond to $WO_6$ constituting the core POM structure with red circles indicating oxygen atoms and, "P" circled in green showing phosphorus atoms); (inset top middle) theoretical isotopic pattern (gray trace) of the $[POMc12 + Al]^-$ species in the region of the molecular ion at a resolving power of 10,000

aluminum chloride, the MALDI mass spectrum of POMc12 (Figure 1) displays an abundant and unique molecular ion species $[POMc12 + Al]^-$; this cation was thus chosen to optimize sample preparation. Molar ratios of $Al^{3+}$:POMc12 between 10 and 1000 provided similar results (data not shown). A ratio below 10 did not induce sufficient adduct ion formation, whereas ratios higher than 1000 led to salt precipitation in the apolar solvents. The final three-component ratio of (matrix):(added cations):(analyte) was approximately of 1600:160:1 for mixes containing one salt, or 1600:80:1 for mixes containing two added salts (each salt present in a proportion of 80). An excess of cations served to ensure the production of the desired abundant intact POM adduct ion. Notably, two different MALDI plates were used during our analyses: one made of stainless steel and the second an isolating polymer (see Experimental section). The results were quite comparable for the two plates. Fragmentation yield and, more generally, signal intensities, were higher on the polymer plate, but no clear intact species desorption trends or in-source fragmentation trends could be correlated to the plate composition. Herein, all the presented results were obtained using a stainless steel MALDI plate.

## *Two Categories of Matrixes: Group 1 and Group 2*

The model POMc12 analyte provided signals over a wide range of matrixes having quite different characteristics. Spectral patterns varied depending upon the matrix but, consistently, tungsten-containing peaks in the molecular ion region were observed. The 11 tested matrixes can be separated into two groups according to their ease in producing molecular adduct ions and to induce in-source fragmentations. Typically, as shown in Figure 2, an abundant molecular species was observed in the presence of $Al^{3+}$, such as $[POMc12 + Al]^-$ at *m/z* 2902, as well as many fragment ions. POM fragments are easily identified because of the tungsten isotopic signature. The first group of matrixes includes CNA, IAA, HABA, DAN, DIT, DCTB and CHCA; these matrixes all offer MALDI mass spectra characterized by abundant intact adduct ion signals and also readily observable in-source fragmentations when the laser power was increased (Figure 2). The intact adduct ion is sometimes accompanied by other weak unresolved signals corresponding to different types of adducts, observable in Figure 2 in the region of the intact adduct ion $[POMc12 + Al]^-$. The second group of matrixes contains DHB, SA, FA, THAP, and HPA (data not shown). These matrixes provide MALDI mass spectra with multiple signals in the molecular ion region at high laser fluence. However, unlike the first group, an increase of the laser power did not lead to observable fragment ions (i.e., no in-source decay, ISD was observed).

## *MALDI In-Source Decay (ISD) of POMc12, Mechanism of Decomposition*

Fragment ions observed by decompositions of POMc12 are divided into two parts. The first part concerns high mass

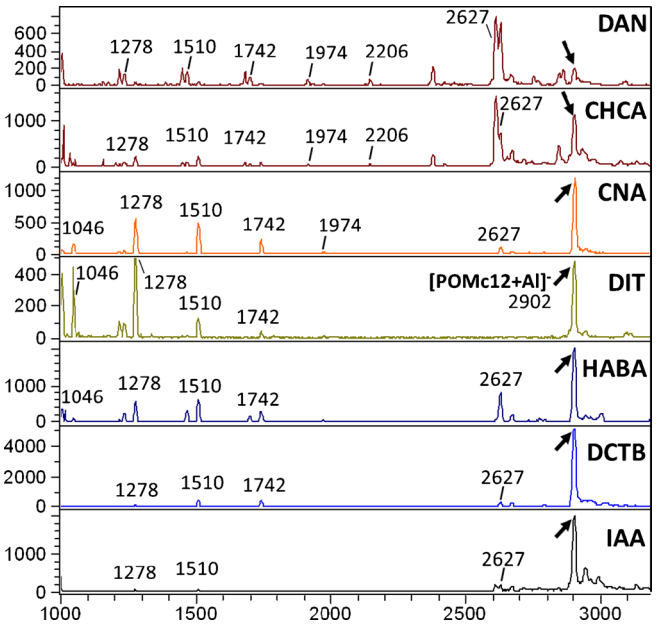


**Figure 2.** Negative ion MALDI mass spectra of POMc12 in the presence of $Al^{3+}$ using a laser power of 1.5 times that of the laser threshold. Results are shown for seven different matrixes, each present at a concentration of 10 g/L with 5 mM $AlCl_3$; 1 µL was deposited on the stainless steel plate. The $[POMc12 + Al]^-$ ion appears at *m/z* 2902 and its presence is indicated by an arrow in each spectrum

fragments (*m/z* >2500) which still contain a portion of the organic functionalization. Among these decomposition products, the fragment ion centered at *m/z* 2627 $[HSiW_{10}O_{34}POC_{12}H_{25}]^-$ corresponds to the loss of one alkylphosphonium group ($[O_3PC_{12}H_{25}]^{2-}$). This fragment ion is observed for all targets (Figure 2), whatever the Group 1 matrix used (i.e., CNA, IAA, HABA, DAN, DIT, DCTB and CHCA). This *m/z* 2627 fragment appears in variable relative intensity and could possibly include a contribution from product degradation occurring at the moment of target preparation, instead of being produced during the MALDI process. Among the matrix-dependent fragments observed in the *m/z* 2500–2850 range, the highest *m/z* detected fragment ion (*m/z* 2860) corresponding to $[POMc12\text{-}O + H]^-$ was observed only with DAN and CHCA as matrix.

The second type of fragment ions corresponds to those that are detected below *m/z* 2000 (Figure 2). These fragments, observed especially at elevated laser powers, are produced through prompt in-source dissociations, also known as in-source decay (ISD). ISD has been mainly reported for peptides and proteins and ISD experiments on peptides mainly display c and z in-source fragments [26]. Such sequencing fragment ions were produced through radical fragmentation processes as demonstrated by hydrogen/deuterium transfer [27]. Similarly, dissociations of benzyl-pyridines used as thermometer molecules were explained through two fragmentation mechanisms, one similar to peptide fragmentation [28] and the other by a thermal dissociation route [26]. For the investigation of glycans, ISD produced hydrogen abstraction (still as $H^{\bullet}$) [29]. ISD experiments are often successful at producing abundant

fragments when DHB, SA or DAN are employed [30, 31]. These matrixes exhibit a propensity to readily provide $H^{\bullet}$ during the MALDI process and this possibility can induce extensive in-source fragmentations. Thus, matrix selection is an important parameter for ISD experiments, and the tendency of a given molecule toward fragmentation is clearly matrix-dependent [32].

In examining the matrixes of the first group characterized by abundant in-source fragment ions in our experiments, the matrixes listed (except for DAN [33]) are not usually considered to be efficient in generating ISD on more commonly encountered analytes (e.g., peptides). For example, the widely used CHCA matrix that offered particularly extensive in-source fragmentations in our MALDI experiments is usually considered to be an inefficient matrix for promoting ISD [30, 34–36]. However, the CHCA matrix found an appreciation as the most efficient matrix to provide metastable dissociations of peptides or proteins during so-called post-source decay (PSD) experiments [27]. The kinetics of PSD and ISD processes are quite different [28]. ISD is a prompt process leading to direct fragmentation in the ion source, as opposed to PSD, which leads to the production of metastable fragment ions that are produced/appear only after leaving the ion source (some tens of microseconds following the laser shot). ISD fragments are formed promptly during the first nanoseconds in the MALDI plume or even earlier during laser irradiation, while analyte molecules are still in the crystalline solid [37]. Such prompt fragmentations found a coherent explanation in the proposed radical origin of these processes, which can also rationalize the matrix dependence of the decomposition behavior. Hydrogen radical donating abilities of various matrixes have been measured [30] and results show that DHB or DAN matrixes are capable of providing $H^{\bullet}$ much more readily than CHCA. Conversely, PSD is a much slower dissociation process induced by vibrational energy uptake of the analytes, similar to the energy uptake occurring in collision induced decomposition (CID) processes [38].

The fragmentation mechanism of POMc12 with its oxometallic core coordination structure cannot be compared with peptides that have a linear primary structure. The origin of the observed facile fragmentations in POMs is thus likely to be different from the radical-induced process that operates for peptides. We thus consider that hydrogen radical transfer is not a major factor in ISD of POMc12 because most of the matrixes observed to induce in-source fragmentations in our experiments are not efficient providers of $H^{\bullet}$ (e.g., CHCA, CNA, DCTB).

To further investigate the POM fragmentation processes, MS/MS through LIFT experiments [39], which invoke similar processes as post-source decay (PSD) [32], were performed for POMc12 adduct ions, but no fragmentations were observed. The molecular adduct ion, comprised of POMc12 and cations, thus seems to either fragment suddenly (ISD), even with 0 ns of extraction delay time value, or remain intact over the metastable time scale. MS/MS experiments using low-energy CID (performed on a MALDI-LTQ Orbitrap, Thermo Scientific) also showed no significant fragmentation. However, MS/MS experiments acquired on a TOF-TOF permitting access to high-energy collisions (1 keV) gave fragment ions similar to those observed in ISD spectra (Figure 3). Thus, POMc12 ISD fragments could be considered as fragments originating from prompt processes involving electronic excitation, which is consistent with the fact that matrix molecules may access excited electronic states upon laser photon absorption [40]. Moreover, due to the presence of the transition metal atoms (tungsten) that are quite capable to accumulate electrons upon minor structural reorganization [10], we can rationalize why the presence of radical hydrogens does not promote fragmentations (e.g., DHB and SA induce extremely low ISD for POMc12 fragments, contrary to what has been observed for analyte biological molecules [41]).

Electron emission is a well-documented occurrence in MALDI, and the matrix itself can be a supplier of electrons, as can be the MALDI plate surface [42]. In the case of CNA, the only matrix ions observed in the mass spectrum are $CNA^{\bullet-}$/$CNA^{\bullet+}$ (see Supplementary Materials, Figure S2). In an attempt to clarify the role of electrons in fragmentation processes, an electrically insulated polymer plate was used as the MALDI support. Surprisingly, the level of fragmentation and the presence of fragments containing an extra electron were even higher when using the insulated plate (see Supplementary Materials, Figure S3). We conclude that the ISD fragmentation process is not being driven by electronic emission from the plate.

## *Calculation of ISD Fragment Yields and Ranking of Matrix Propensity Toward Fragmentation*

To obtain a measure of the matrix-dependence of POMc12 toward ISD, the fragmentation yields were calculated by con-

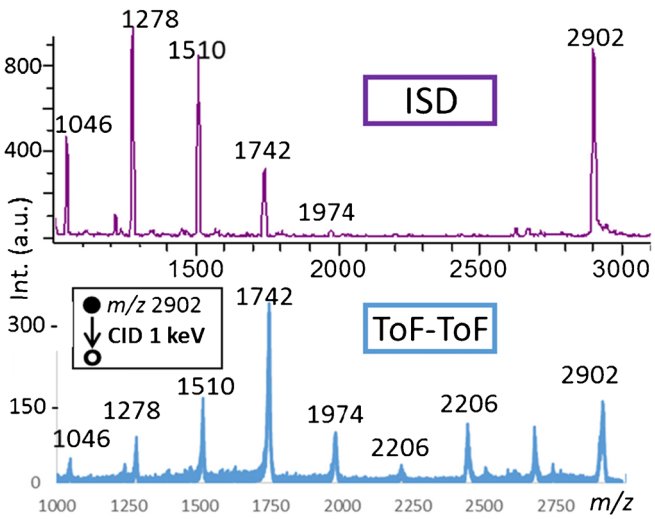


**Figure 3.** MALDI ISD (top) and MALDI TOF/TOF (bottom) mass spectra of the mix POMc12/$Al^{3+}$/CNA. For ISD, laser power was set to 1.5 × threshold, whereas for TOF/TOF, CID collision energy was set to 1 keV with the precursor mass window set to transmit *m/z* [2887–2912]

sidering the peak areas of all the signals observed between $m/z$ 1000–3500 according to the following equation: $\frac{\sum(peaks\ areas\ of\ fragments\ ions)}{\sum(peaks\ areas\ of\ all\ the\ ions)}$. Ions issued from POMc12 fragmentation are readily recognized because of their characteristic isotopic patterns. However, due to the broad distribution of isotopic peaks, it is not easy to sum all the peak areas of the minor peaks, so only the most abundant peaks in each isotopic pattern were considered (i.e., between five to eight central peaks). The exact number of peaks considered in the calculation depends upon the width of the isotopic distribution (i.e., it is directly dependent on the number of tungsten atoms present). To integrate the same proportion for each ion signal, at least 50% of the total peak area was employed. All theoretical ion isotopic patterns were modeled to determine how many central peaks correspond to 50% of the theoretical total area. The number of peaks, the area of which must be summed, is reported in Table 1.

Based on the calculated values given in Table 2, a relative ranking of the ability of a tested matrix to induce POM ISD fragmentation can be given as: DAN > CHCA > CNA > DIT > HABA > DCTB > IAA. This ranking differs substantially from the one proposed for matrixes inducing ISD fragmentation of peptides via a hydrogen radical transfer mechanism [27–31]. The fragmentation yield values showed a large variation even for two matrixes, CNA and DCTB, which might be considered to have similar properties (i.e., they are both aprotic and each exhibits low polarity). In addition to the values presented in Table 2, for the remaining five tested matrixes (i.e., DHB, SA, FA, THAP and HPA) in-source fragments were not observed in sufficient abundances to offer a reliable calculation of fragmentation yield; suffice it to say that they were all near "0". The fragmentation yield varies not only as a function of the employed matrix but also upon the laser power. For the matrixes CNA, DIT, HABA, DCTB, and IAA the fragmentation yield increases with laser power, whereas CHCA and DAN show rather constant fragmentation yield values from the threshold laser power to higher laser power values [43]. Owing to the unusually broad variety of matrixes allowing POMc12 ionization and the production of in-source fragments, it seems that chemical properties, such as acidity or electron affinity, do not play a predominant, determinant role in POMc12 MALDI ionization. However, the affinity of the analyte for an available cation could play a crucial role in the production of a preferred molecular adduct ion. In a situation where a dominant cation was observed (for example with $Al^{3+}$), changing the matrix (resting within the first group) had little impact on the produced ions. That is to say, the matrix affinity for a specific cation was not observed to influence the obtained results but rather, free cation attachment was claimed to be the predominant process leading to ion formation [21].

The second group of matrixes (i.e., DHB, HPA, SA and FA) required higher laser powers to give optimal signals, and we speculate that this is due to an increased difficulty to desolvate the molecular adduct ion upon desorption. This second group of matrixes showed no in-source fragmentations whatsoever, and only a variety of low-level signals were observable above the molecular mass, indicating that the expected specific adduct ions were less promoted or disfavored.

Among all of the matrixes of the first group, follow-up studies focused on the use of CNA. This matrix allows the observation of highly resolved peaks for intact molecular adduct ions and fragments ions at high S/N values compared with spectra obtained using other matrixes under identical instrumental conditions. The CNA matrix produced mainly a single high-abundance molecular adduct ion at just above the threshold laser power value. Compared with DAN or CHCA, which display higher fragmentation yield values, CNA preferentially induces the production of low mass fragments possessing less than 8 tungsten atoms (see Table 2). CNA induced higher in-source fragmentations than DIT, HABA, DCTB and IAA at laser power values of 1.5 times the laser threshold. As shown in Table 2, use of the CNA matrix resulted in the highest resolution spectra either for the molecular adduct ion, or for fragment ion signals, regardless of the laser power used.

## *Competition for Cation Attachment: Evaluation of POMc12's Affinity for Various Cations*

Despite some previous work investigating the affinities of cations for a variety of analytes in the positive ion mode [41], we are not aware of any studies investigating cation affinities for polyanionic species. We thus embarked on studies to probe the possibility of preferential attachment of cations to polyanions. Shown in Figure 4 are the MALDI mass spectra of POMc12 acquired in the presence of various cations introduced into the CNA matrix. No matter which cation was introduced in the matrix mixture, a clear modification of the spectral allure indicated that each cation influenced the spectral profile, often including the production of the molecular adduct as a singly charged ion of the form: $[POMc12 + cation(s)]^-$. Among the cations tested, $Fe^{3+}$, $Al^{3+}$, $Ga^{3+}$ and $Li^+$ allowed the formation of intense molecular adduct ion signals, whereas addition of $Cr^{3+}$, $Cu^{2+}$, $Co^{2+}$, or $Mn^{2+}$ resulted only in a variety of low abundance adducts such as $[POM + CuH/CoH]^-$ or $[POM + 2Cu/2Co]^-$, and numerous other difficult-to-assign overlapping signals in the molecular ion region. Additions of $Mg^{2+}$, $Na^+$, or $K^+$ led to MALDI spectra that displayed weak signals and often mixtures of signals in the high mass region (results not shown).

**Table 1.** Number of peaks in a given isotopic cluster used to calculate the in-source fragmentation yield

| | | | | | |
|---|---|---|---|---|---|
| Number of W in the ion | 4 | 5 | 6 | 7 | 10 |
| Number of peaks integrated to reach 50% of total signal's area | 5 | 5 | 6 | 6 | 8 |

**Table 2.** Fragmentation yield and peak resolution in the region of the molecular adduct ion at 1.5 × threshold laser power. Mixtures consisted of matrix at 10 g/L in ternary solvent with 5 mM $AlCl_3$

| Matrix | DAN | CHCA | CNA | DIT | HABA | DCTB | IAA |
|---|---|---|---|---|---|---|---|
| Fragmentation yield | 0.89 | 0.59 | 0.47 | 0.36 | 0.31 | 0.09 | 0.04 |
| Peak resolution on $[POM + Al]^-$ | 3000 | 2000 | 4000 | 2000 | 3000 | 2500 | 2000 |
| Peak resolution on $[SiW_5O_{17}Al]^-$ | 6000 | 3000 | 7000 | 3000 | 7000 | 3000 | 4000 |

Even if most trivalent cations (i.e., $Fe^{3+}$, $Al^{3+}$, $Ga^{3+}$) display abundant singly charged $[POM + cation]^-$ signals, as might be expected for such quadruply negatively charged POM species, the trend cannot be explained simply on the basis of cation charge because another trivalent cation (i.e. $Cr^{3+}$) shows a very poor propensity for POM attachment. In evaluating the alkali metals and their affinities for the polyanionic POM, $Li^+$ gave very satisfactory results producing an abundant $[POM + 3Li]^-$ signal, whereas $Na^+$ and $K^+$ do not result in the detection of analogous resolved species in the molecular ion region. When two salts were introduced simultaneously, the molecular adduct ion signal generally revealed a preferential interaction of POMc12 for one of the two cations. For instance, the mixture of $Ga^{3+}$ and $Al^{3+}$ led only to the observation of the singly charged $[POMc12 + Al]^-$. In a direct comparison of $Al^{3+}$ versus $Fe^{3+}$, exclusive formation of a specific adduct species was demonstrated by placing 10 times more $Al^{3+}$ than $Fe^{3+}$ in the sample preparation (matrix/$Al^{3+}$/$Fe^{3+}$/POMc12 ratio 1500/150/15/1); despite the disadvantage in terms of concentration, ionic molecular species containing uniquely Fe(III) were observed. However, mixtures of divalent and monovalent cations can provide both mixed and single cation-containing adduct species. For example, the mixture of $Co^{2+}$ + $Li^+$ produced two main species by MALDI: $[POMc12 + 3Li]^-$ and $[POMc12 + Li + Co]^-$ (see Figure 4); however, it is possible to rank these two cations ($Li^+$ and $Cu^{2+}$) by performing a comparison with a third cation, $Ga^{3+}$. Gallium has a higher affinity for POMc12 than $Cu^{2+}$ but lower than $Li^+$.

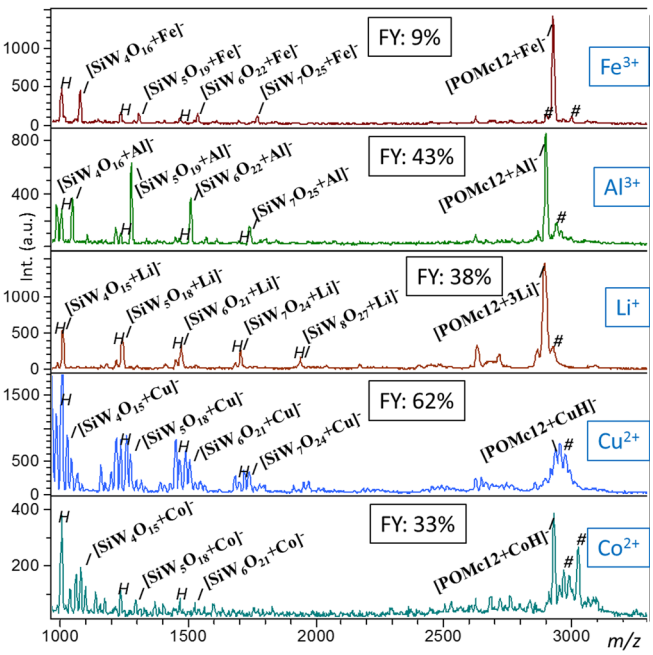


**Figure 4.** MALDI spectra of POMc12 in CNA with different cationic species and calculated fragmentation yield at high laser power (1.5 × threshold). Spectra were acquired in reflectron mode from 200 laser shots. Product ion formulas are given for the most abundant peaks. Unresolved and/or low abundance molecular adduct ions are labeled with "#"; ions containing hydrogen are marked as "*H*". Calculated fragmentation yield (FY) is given for each sample preparation

These combined observations allowed us to create a relative ranking of POMc12 affinity toward various cations. The relative affinity classification can be constructed as: $Fe^{3+}$ > $Al^{3+}$ >$Li^+$> $Ga^{3+}$>$Co^{2+}$ >$Cr^{3+}$>$Cu^{2+}$> [$Mn^{2+}$, $Mg^{2+}$] > [$Na^+$, $K^+$]. Owing to poor quality spectra obtained with the mixture of $Mn^{2+}$ and $Mg^{2+}$, or $Na^+$ and $K^+$, it was more difficult to precisely rank their abilities to form adducts with the model POM. This competition for cation attachment can help to shed light on the ionization mechanism. It was observed that the POMc12 is clearly able to choose one or more preferred cation(s) to form the singly charged ionic molecular species. This indicates that upon desorption, the analyte has access to a variety of cations in its surroundings. From the available cationic species, preferred adducts are formed, possibly upon decomposition of the aggregates desorbed during the MALDI process that are known to be very large [5], and are thus capable of containing numerous cations. On the other hand, POMs are known to precipitate and form crystalline structures with alkali or ammonium counter-ions. For this reason, it seems improbable to us that the adduct species observed in MS spectra are "pre-formed" in the matrix crystal, as proposed by the "Lucky Survivor" model [44]. We thus consider that the formation of the singly charged adduct molecular ions rather occurs by cation exchange in the plume (i.e., during decomposition of the initially formed aggregates). In order to gain insight into the desorption/ionization mechanism, and to distinguish between cation exchange occurring in the gas phase versus in the matrix crystal, additional experiments were performed based upon the use of two distinct (solid) matrix preparations. The first was prepared by mixing and drying a solution of CNA, POMc12, and a cation displaying a low affinity for the POMc12 analyte, whereas the second was prepared by mixing solutions of only CNA matrix and a cation of higher affinity (e.g., Fe) in the absence of the POM. Afterwards, the two dry, crystallized mixtures were blended in the solid state using a clean spatula, and this mixture was deposited

on the MALDI plate. In this way, no "pre-formed" [POMc12 + cation of higher affinity] complex is expected to exist in the matrix bulk. The resulting MALDI mass spectra (Figure 5) demonstrate, however, that even when the higher affinity cation is not present in the matrix crystal, if it is desorbed into the gas phase simultaneously with, and in close proximity to, the analyte (i.e., leading to the analyte and the higher affinity cation co-existing in the plume), the [POMc12 + cation of higher affinity] adduct species is indeed observed in the spectrum. These experimental observations indicate that production of preferred, higher affinity adduct species takes place in the gas phase, most likely during the early stages of plume expansion, as opposed to being "pre-formed" on the target. It should be noted that the intensity of the [POMc12 + cation of higher affinity] complex varies as the laser shot location is changed, which is consistent with what one would expect for this type of nonhomogeneous target.

Variation in the signal intensity of the adduct species as a function of the particular cation participating in adduction has been previously reported in MALDI-MS [41]. In assessing POMc12 interactions with cations, no overwhelming trend can be drawn from the MALDI mass spectra concerning a preferred valence of the cation. Nevertheless, it was noticed that cations characterized by smaller radii do exhibit an increased tendency to form abundant molecular adduct species. The radii of cations such as $Al^{3+}$ (54 pm), $Li^{+}$ (76 pm), or $Cu^{2+}$ (73 pm) [45] that efficiently form adducts with POMc12 and exhibit large signals in mass spectra are much smaller than those of the other alkali metals (e.g., $Na^{+}$, $K^{+}$, whose radii exceed 100 pm) that provide poor MALDI results, or even $TMA^{+}$, which was never observed as an adduct on POMc12 during our MALDI experiments. To test whether the cation affinity trend was more general in nature, ESI experiments were undertaken to ascertain whether those cations exhibiting strong affinities for POMc12 in MALDI would perform equally well in electrospray ionization (ESI). Somewhat surprisingly, the use of ESI did not result in the observation of any species entailing lithium or aluminum adduction to the model POM. However, this result is in line with that of Deery et al. [46], who also observed divergent behaviors for MALDI-MS and ESI-MS analyses of polystyrene cationic adducts. In addition, the little NMR data pertaining to characterization of POMc12 in solution [19] establishes the proximity of counter-ions $TMA^{+}$ or $K^{+}$ to POMc12 in the liquid phase, but no NMR characterization has been performed in the presence of cations such as $Fe^{3+}$ or $Li^{+}$. Notably, results derived from in-solution conditions may not be applicable to a solid matrix such as that which constitutes the MALDI target.

In competition experiments, lithium revealed a specific behavior in many respects. In terms of the molecular signal obtained in the presence of lithium, very wide isotopic patterns were obtained (Figure 6). These extended isotopic distributions were explained by the presence of various overlapping adduct ions incorporating two (with one additional $H^{+}$), three, or even four lithiums. The appearance of unexpected $[POMc12 + 4Li]^{-}$ species demonstrated the existence of electron capture processes. This phenomenon was not restricted to lithium addition only; it was also observed for a mixture of lithium with $Fe^{3+}$ or $Al^{3+}$ cations, from which the mixed adduct species $[POMc12 + FeLi]^{-}$ and $[POMc12 + AlLi]^{-}$ were detected at the same time as the expected adduct with the trivalent cation. Similarly, the peak isotopic pattern of the detected molecular adduct ions in the presence of a mixture of $Fe^{3+}$ and $Li^{+}$ is noticeably wider than the corresponding one for $Al^{3+}$ and $Li^{+}$ (Figure 5). This points to a higher abundance of lithiated species in the case where iron is present. Parenthetically, POMc12 is undetectable in the positive mode except in the presence of lithium and with high laser power, which enabled observation of a weak signal corresponding to $[POMc12 + 5Li]^{+}$. The unusual behavior observed when lithium is used (i.e., the presence of molecular adduct ions revealing electron capture) is not explicable by the possibility to reduce the lithium, which has a very high reduction potential. We also noticed in Figure 6 that the proportion of species with an extra lithium, so necessarily also an extra electron (i.e., $[POMc12 + FeLi+e^{-}]^{-}$ or $[POMc12 + AlLi + e^{-}]^{-}$), is higher in the case of $Fe^{3+}$ than with $Al^{3+}$. This indicates that the attaching cation influences the ease with which the complex can accommodate an arriving electron.

## *Presence of Cations in Fragment Ions of POMc12*

The common feature of fragments of POMc12, observed either by high energy collisions or ISD conditions, is that they remain

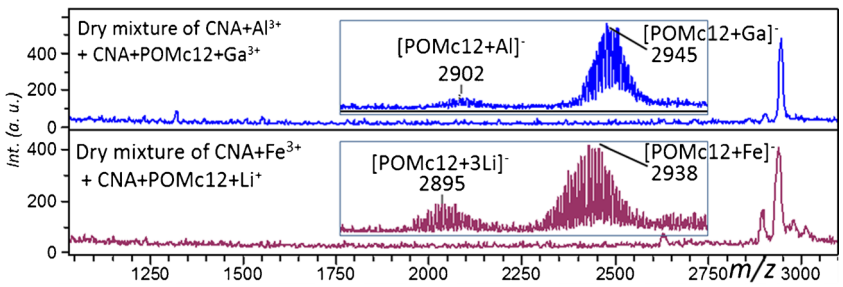


**Figure 5.** MALDI spectra produced from dry mixture blending of two different solid matrix preparations; (top) mixture of crystals formed by dried droplet from a preparation of CNA + POMc12 + $Ga^{3+}$ mixed dry with dry CNA+$Al^{3+}$; (bottom) dry crystals of CNA + POMc12 + $Li^{+}$ mixed with dry CNA + $Fe^{3+}$. Each spectrum represents the sum of 500 laser shots and each was acquired at threshold laser power

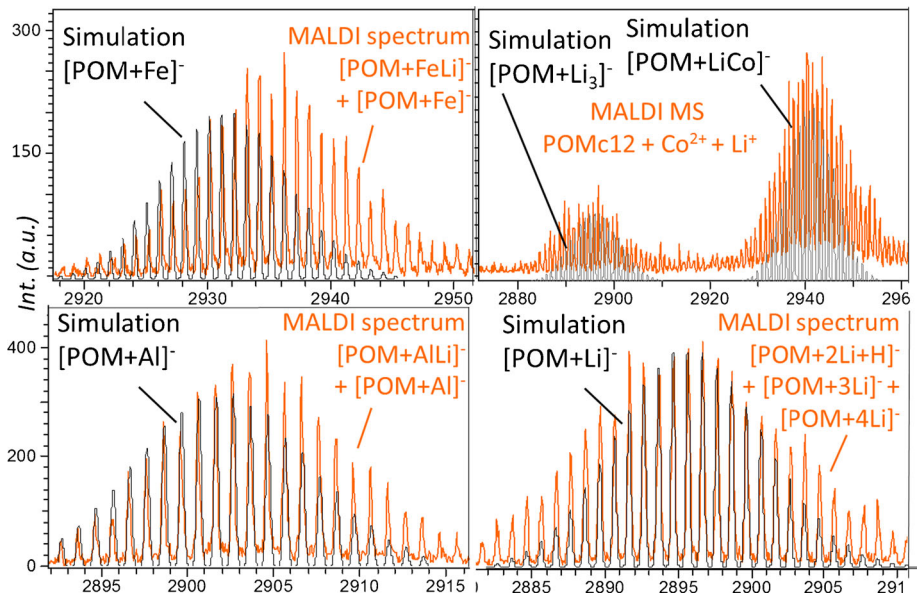


**Figure 6.** Comparison of MALDI mass spectra (orange traces) and theoretical isotope distributions (black traces) of various intact singly-charged adducts of POMc12. Many species revealed electron capture as evidenced by the observation of four positive charges adducted with POMc12

singly charged anions, but a rather diverse array of fragmentation pathways is observed depending upon the cation forming the adduct and its valence. Whatever the cation used, including those that did not display abundant molecular species such as $Mg^{2+}$, $Na^+$, $K^+$ and $Mn^{2+}$, many of the observed fragments contained cations. Formulas of observed fragments are detailed in Table 3, where a few examples of each type of cation are presented, but note that the formulas of fragments obtained for a given valence of cation are analogous to those of another cation of the same valence (e.g., $Al^{3+}$ and $Fe^{3+}$, or $Na^+$ and $Li^+$). Core fragments obtained without salt introduction contained either the core structure alone, or the core structure with added protons. These fragments are observed, although often in low abundance, for each cationic mixture. When singly charged alkali metal cations (i.e., $Li^+$, $Na^+$, or $K^+$) are introduced, the nature of the core fragment does not change: alkali metal cations simply replace the protons that would attach in the absence of the added salts. A common element observed in fragmentation spectra obtained in the presence of a wide variety of cations is the tendency to observe series of fragments that differ by the mass of a $WO_3$ moiety (232 Da neutral, see Figure 4 and Table 3). This result is somewhat similar to a previous report that showed a series of MALDI-MS fragments containing different numbers of Mo moieties (i.e., $[Mn_6Mo_{10}]$ to $[Mn_6Mo_4]$) for a hybrid POM containing a polyoxomolybdate core [14]. In that study, the authors used the information contained in the MALDI mass spectrum of the $(Mn_6Mo_{10})$ hybrid species in order to try to gain insight into its formation in solution.

For POMc12, when triply charged cations, such as $Al^{3+}$, $Fe^{3+}$, $Cr^{3+}$ and $Ga^{3+}$ are employed, fragments observed contain an extra oxygen compared with the ones observed when adding singly charged cations [e.g., $(SiW_5O_{19}Ga)^-$ instead of $(SiW_5O_{18}Li)^-$]. Despite the variety of fragment ion compositions, all of these species remain globally singly charged under MALDI conditions. For doubly charged cation addition (considering only Co and Cu because Mn and Mg did not display enough signal to be interpreted), however, two different outcomes are observed in MALDI mass spectra. Some POM fragments contain the divalent cation plus a proton (a

**Table 3.** Abundant ions observed from a mixture of $[SiW_{10}O_{36}(POC_{12}H_{25})_2]^{4-}$ and various cations as a function of the number of tungsten atoms (#W) contained in a fragment. Results for addition of $Li^+$, $Al^{3+}$, and $Co^{2+}$ cations are presented, along with those for the POM without any added salt (Ø). Underlined fragments represent species that have undergone a one-electron reduction. Fragments observed with zero cations incorporated invariably represent low abundance signals

| #W | 4 | 5 | 6 | 7 | 10 | Molecular adduct ion |
|---|---|---|---|---|---|---|
| Ø | $[SiW_4O_{15}H]^-$<br>$[\underline{SiW_4O_{14}}]^-$ | $[SiW_5O_{18}H]^-$<br>$[\underline{SiW_5O_{17}}]^-$ | $[SiW_6O_{21}H]^-$<br>$[\underline{SiW_6O_{20}}]^-$ | $[SiW_7O_{24}H]^-$<br>$[\underline{SiW_7O_{24}H}]^-$ | $[HSiW_{10}O_{34}POC_{12}H_{25}]^-$ | Mix unresolved |
| $Li^+$ | $[\underline{SiW_4O_{15}Li}]^-$ | $[\underline{SiW_5O_{18}Li}]^-$ | $[\underline{SiW_6O_{21}Li}]^-$ | $[\underline{SiW_7O_{24}Li}]^-$ | $[LiSiW_{10}O_{34}POC_{12}H_{25}]^-$ | $[POMc12 + 3Li]^-$ |
| $Al^{3+}$ | $[SiW_4O_{16}Al]^-$<br>$[W_4O_{14}Al]^-$ | $[SiW_5O_{19}Al]^-$<br>$[W_5O_{17}Al]^-$ | $[SiW_6O_{22}Al]^-$<br>$[W_6O_{20}Al]^-$ | $[SiW_7O_{25}Al]^-$ | $[HSiW_{10}O_{34}POC_{12}H_{25}]^-$ | $[POMc12 + Al]^-$ |
| $Co^{2+}$ | $[SiW_4O_{16}HCo]^-$<br>$[\underline{SiW_4O_{15}Co}]^-$<br>$[\underline{W_4O_{13}Co}]^-$ | $[SiW_5O_{19}HCo]^-$<br>$[\underline{SiW_5O_{18}Co}]^-$ | $[SiW_6O_{22}HCo]^-$<br>$[\underline{SiW_6O_{21}Co}]^-$ | $[SiW_7O_{25}HCo]^-$<br>$[\underline{SiW_7O_{24}Co}]^-$ | $[\underline{CoSiW_{10}O_{34}POC_{12}H_{25}}]^-$ | $[POMc12 + CoH]^-$<br>$[POMc12 + 2Co]^-$<br>mix |

"trivalent-like" cation), the elemental composition of which is similar to that observed in the presence of a triply charged cation (e.g., $[SiW_4O_{16}CuH]^-$ has the same core structure as $[SiW_4O_{16}Fe]^-$). The second type of fragment ion has captured an electron, so the integrated divalent cation is included effectively as a monovalent cation (e.g., $[SiW_4O_{15}Cu]^-$ has the same core structure as $[SiW_4O_{15}Li]^-$). Electron capture could be either considered as the reduction of the cation or the reduction of the core POM; this type of reduction has been commonly observed for Cu(II) [47], but it is more surprising to also observe this behavior for fragments containing Co(II).

### *Analyses of Other POMs Using CNA as the MALDI Matrix*

The optimized target preparation method was applied to other functionalized POMs with different charge states, such as species of the following molecular formulas: $(PW_{11}O_{39}[GePhCCPhN3])^{4-}$ or $(PW_{11}O_{39}[SnPhI])^{4-}$ or $(SiW_9O_{34}[POC_{12}H_{25}]_2)^{6-}$ synthesized with $TMA^+$, $Na^+$, or $K^+$ as counter ions [48]. For these functionalized POMs, in-source fragments were observed in preference to molecular species. The most successful analyses, with respect to POMs of similar structure to POMc12, were performed for $TMA_3K(SiW_{10}O_{36}[POC_{10}H_{21}]_2)$, $TBA_3K(SiW_{10}O_{36}[POC_8H_{17}]_2)$, and $TBA_3K(SiW_{10}O_{36}[POH]_2)$ that differ only by the length of the attached alkyl side chains (see Supplementary Materials, Figure S4). In addition, the non-functionalized POM $K_3[PW_{12}O_{40}]$ also gave useful results (see Supplementary Materials, Figure S5). In the presence of LiCl or NaCl, introduced in matrix solutions, the anions $[PW_{12}O_{40}+2Li]^-$ or $[PW_{12}O_{40}+2Na]^-$ were easily detected. This inorganic compound could be ionized by laser desorption ionization (LDI), i.e., without matrix addition, employing a high laser fluence. Yet, LDI spectra display, even in the presence of added LiCl, only $PW_{12}O_{39}^-$ ions (having undergone loss of one oxygen atom). The fact that POMs are not "electron sensitive" (i.e., they can stock and release electrons without further decompositions [10]), could be an important factor in promoting their survival in the plume, rich in matrix radical anions and cations.

## Conclusion

Polyanionic polyoxometalates (POMs) have been successfully analyzed using MALDI-MS in the negative ion mode. Sample matrix optimization established that the matrix 9-cyanoanthracene (CNA), in the presence of an excess of cations, provided efficient analyses (intense and highly resolved peaks) either for singly charged intact POMc12 anions, or for in-source fragments when the laser power was largely increased. Comparing a first group of matrixes: CNA, IAA, HABA, DAN, DIT, DCTB, and CHCA to a second group: DHB, SA, FA, THAP, and HPA, we observed that the first group offers both more abundant intact singly charged anionic adducts and prevalent in-source fragmentations at elevated laser powers that are absent when employing the second group. The ability to induce in-source fragmentations was found to vary as a function of the employed matrix, thereby allowing us to establish a ranking of the matrixes starting with those that exhibit facile fragmentation to those that offer limited or no ISD: DAN > CHCA >CNA> DIT > HABA > DCTB > IAA > [DHB, SA, FA, THAP, HPA]. We postulate that the first group of matrixes enables a higher level of energy uptake to POM species, thereby permitting an initial higher level of desolvation and eventually access to endothermic decompositions that are not accessible when employing the second group of matrixes. The observed prompt fragments are proposed to originate from transferred energy derived from initial electronic excitation of the matrix, which rationalizes the increase in ISD with rising laser power. We postulate that this energy is rapidly converted to vibrational energy that leads to prompt decompositions in the MALDI source. POMs are known for their capability to sequester and release electrons, and this property is exhibited in negative ion mass spectra that reveal molecular ions that have obligatorily accepted an electron.

Experiments designed to assess the competition of various cations toward adduct formation with POMc12 have enabled the construction of the following affinity ranking of POMc12 towards cations: $Fe^{3+} > Al^{3+} > Li^+ > Ga^{3+} > Co^{2+} > Cr^{3+} > Cu^{2+} > [Mn^{2+}, Mg^{2+}] > [Na^+, K^+]$. This experimental affinity ranking reflects, at least in part, a gas-phase competition for attachment to the polyanionic POM that occurs prior to any fragmentation process. The observed "high affinity" adduct species are produced during the early stages of plume expansion as demonstrated by the observation of high affinity complexes from initial mixtures comprised of two matrix crystal preparations: the first containing only low affinity complexes with POMc12, and the second containing only the higher affinity salt. We additionally observe that in the vast majority of cases, formed fragment ions contain the cations with the strongest affinities for the polyanionic POM. This finding corroborates our conclusion that Group 1 matrixes permit thermal desorption of POM-containing aggregates that contain sufficient energy to permit movement and attachment of preferred cations, and to allow complete desolvation of cation-bearing, singly charged anionic POMs. If sufficient energy is made available at augmented laser powers, prompt fragmentation of these adducts can ensue.

## Acknowledgments

The authors especially thank our colleagues Drs. Vincent Jallet and Geoffrey Guillemot and Pr. Anna Proust from the E-POM group of the IPCM laboratory for the POM products that they graciously provided. The authors also thank Dr. Joëlle Vinh for allowing them to perform experiments on the MALDI-Orbitrap at the ESPCI.

## References


1. Harvey, D.J.: Analysis of carbohydrates and glycoconjugates by matrix-assisted laser desorption/ionization mass spectrometry: an update for the period 2005-2006. Mass Spectrom. Rev. **30**, 1–100 (2011)
2. Cotter, R.J., Russell, D.H.: Time-of-flight mass spectrometry: instrumentation and applications in biological research. J. Am. Soc. Mass Spectrom. **9**, 1104–1105 (1998)
3. Dreisewerd, K.: Recent methodological advances in MALDI mass spectrometry. Anal. Bioanal. Chem. **406**, 2261–2278 (2014)
4. Karas, M., Krüger, R.: Ion formation in MALDI: the cluster ionization mechanism. Chem. Rev. **103**, 427–439 (2003)
5. Fournier, I., Brunot, A., Tabet, J.C., Bolbach, G.: Delayed extraction experiments using a repulsive potential before ion extraction: evidence of clusters as ion precursors in UV-MALDI. Part I: dynamical effects with the matrix 2,5-dihydroxybenzoic acid. Int. J. Mass Spectrom. **213**, 203–215 (2002)
6. Karas, M., Gluckmann, M., Schafer, J., Glückmann, M., Schäfer, J.: Ionization in matrix-assisted laser desorption/ionization: singly charged molecular ions are the lucky survivors. J. Mass Spectrom. **35**, 1–12 (2000)
7. Knochenmuss, R.: A quantitative model of ultraviolet matrix-assisted laser desorption/ionization including analyte ion generation. Anal. Chem. **75**, 2199–2207 (2003)
8. Gut, I.G.: DNA Analysis by MALDI-TOF mass spectrometry. Hum. Mutat. **23**, 437–441 (2004)
9. Teuber, K., Schiller, J., Fuchs, B., Karas, M., Jaskolla, T.W.: Significant sensitivity improvements by matrix optimization: a MALDI-TOF mass spectrometric study of lipids from hen egg yolk. Chem. Phys. Lipids **163**, 552–560 (2010)
10. Proust, A., Thouvenot, R., Gouzerh, P.: Functionalization of polyoxometalates: towards advanced applications in catalysis and materials science. Chem. Commun. **16**, 1837–1852 (2008)
11. Misono, M.: Catalytic chemistry of solid polyoxometalates and their industrial applications. Mol. Eng. **3**, 193–203 (1993)
12. Ahmed, I., Farha, R., Huo, Z., Allain, C., Wang, X., Xu, H., Goldmann, M., Hasenknopf, B., Ruhlmann, L.: Porphyrin–polyoxometalate hybrids connected via a Tris-alkoxo linker for the generation of photocurrent. Electrochim. Acta **110**, 726–734 (2013)
13. Lubal, P., Koprivová, H., Sedo, O., Havel, J., Lis, S., But, S.: Simultaneous determination of molybdenum(VI) and tungsten(VI) and its application in elemental analysis of polyoxometalates. Talanta **69**, 800–806 (2006)
14. Zhang, L., Clérac, R., Onet, C.I., Healy, C., Schmitt, W.: Towards nanoscopic Mn-containing hybrid polyoxomolybdates: synthesis, structure, magnetic properties, and solution behavior of a {Mn 6 Mo 10 } Cluster. Eur. J. Inorg. Chem. **10–11**, 1654–1658 (2013)
15. Mayer, R., Hervé, M., Lavanant, H., Blais, J.-C., Sécheresse, F.: Hybrid cyclic dimers of divacant heteropolyanions: synthesis, mass spectrometry (MALDI-TOF and ESI-MS), and NMR multinuclear characterisation. Eur. J. Inorg. Chem. **5**, 973–977 (2004)
16. Morgan, J.R., Cloninger, M.J.: Synthesis of carbohydrate-linked poly(polyoxometalate) poly(amido)amine dendrimers. J. Polym. Sci. A Polym. Chem. **43**, 3059–3066 (2005)
17. Wu, Z., Biemann, K.: The MALDI mass spectra of carbosilane-based dendrimers containing up to eight fixed positive or 16 negative charges. Int. J. Mass Spectrom. Ion Processes **165/166**, 349–361 (1997)
18. Robins, C., Limbach, P.A.: The use of nonpolar matrices for matrix-assisted laser desorption/ionization mass spectrometric analysis of high boiling crude oil fractions. Rapid Commun. Mass Spectrom. **17**, 2839–2845 (2003)
19. Jallet, V., Guillemot, G., Lai, J., Bauduin, P., Nardello-Rataj, V., Proust, A.: Covalent amphiphilic polyoxometalates for the design of biphasic microemulsion systems. Chem. Commun. (Cambridge) **50**, 6610–6612 (2014)
20. Hoberg, A., Haddleton, D.M., Derrick, P.J., Jackson, A.T., Scrivens, J.H.: The effect of counter ions in matrix-assisted laser desorption/ionization of poly (methyl methacrylate). European Mass Spectrom. **4**, 435–440 (1998)
21. Zhang, J., Zenobi, R.: Matrix-dependent cationization in MALDI mass spectrometry. J. Mass Spectrom. **39**, 808–816 (2004)
22. Takayama, M.: In-source decay characteristics of peptides in matrix-assisted laser desorption/ionization time-of-flight mass spectrometry. J. Am. Soc. Mass Spectrom. **12**, 420–427 (2001)
23. Boutaghou, N.M., Cole, R.B.: 9,10-Diphenylanthracene as a matrix for MALDI-MS electron transfer secondary reactions. J. Mass Spectrom. **47**, 995–1003 (2012)
24. Breaux, G.A., Green-church, K.B., France, A., Limbach, P.A.: Desorption/ionization mass spectrometry of hydrophobic and hydrophilic peptides. Anal. Chem. **72**, 1169–1174 (2000)
25. Wong, C.K., Chan, T.-W.D.: Cationization processes in matrix-assisted laser desorption/ionization of divalent and trivalent metal ions. Rapid Commun. Mass Spectrom. **11**, 513–519 (1997)
26. Asakawa, D.: Principles of hydrogen radical mediated peptide/protein fragmentation during matrix-assisted laser desorption/ionization mass spectrometry. Mass Spectrom. Rev. (2014)
27. Köcher, T., Engström, Å., Zubarev, R.: Fragmentation of peptides in MALDI in-source decay mediated by hydrogen radicals. Anal. Chem. **77**, 172–177 (2005)
28. Gabelica, V., Schulz, E., Karas, M.: Internal energy build-up in matrix-assisted laser desorption/ionization. J. Mass Spectrom. **39**, 579–593 (2004)
29. Liang, Q., Macher, T., Xu, Y., Bao, Y., Cassady, C.J.: MALDI MS in-source decay of glycans using a glutathione-capped iron oxide nanoparticle matrix. Anal. Chem. **86**, 8496–8503 (2014)
30. Demeure, K., Quinton, L., Gabelica, V., De Pauw, E.: Rational selection of the optimum MALDI matrix for top-down proteomics by in-source decay. Anal. Chem. **79**, 8678–8685 (2007)
31. Asakawa, D., Smargiasso, N., Quinton, L., De Pauw, E.: Peptide backbone fragmentation initiated by side-chain loss at cysteine residue in matrix-assisted laser desorption/ionization in-source decay mass spectrometry. J. Mass Spectrom. **48**, 352–360 (2013)
32. Debois, D., Bertrand, V., Quinton, L., De Pauw-Gillet, M.-C., De Pauw, E.: MALDI-in source decay applied to mass spectrometry imaging: a new tool for protein identification. Anal. Chem. **82**, 4036–4045 (2010)
33. Molin, L., Seraglia, R., Dani, F.R., Moneti, G., Traldi, P.: The double nature of 1,5-diaminonaphthalene as matrix-assisted laser desorption/ionization matrix: some experimental evidence of the protonation and reduction mechanisms. Rapid Commun. Mass Spectrom. **25**, 3091–3096 (2011)
34. Sakakura, M., Takayama, M.: In-source decay and fragmentation characteristics of peptides using 5-aminosalicylic acid as a matrix in matrix-assisted laser desorption/ionization mass spectrometry. J. Am. Soc. Mass Spectrom. **21**, 979–988 (2010)
35. Asakawa, D., Takayama, M.: Cα–C bond cleavage of the peptide backbone in MALDI in-source decay using salicylic acid derivative matrices. J. Am. Soc. Mass Spectrom. **22**, 1224–1233 (2011)
36. Takayama, M., Tsugita, A.: Does in-source decay occur independent of the ionization process in matrix-assisted laser desorption? Int. J. Mass Spectrom. **181**, L1–L6 (1998)
37. Asakawa, D., Calligaris, D., Smargiasso, N., De Pauw, E.: Ultraviolet laser induced hydrogen transfer reaction: study of the first step of MALDI in-source decay mass spectrometry. J. Phys. Chem. B **117**, 2321–2327 (2013)
38. Cotter, R.J., Iltchenko, S., Wang, D.: The curved-field reflectron: PSD and CID without scanning, stepping or lifting. Int. J. Mass Spectrom. **240**, 169–182 (2005)
39. Guaratini, T., Armelini, A.I.P.V., Ferrari, C.R., Schefer, R.R., Neto, A.P., Navas, R., Reigada, J.B., Silva, D.B.: Application of matrix-assisted laser-desorption/ionization time-of-flight LIFT for identification of cocoa condensed tannins. J. Mass Spectrom. **49**, 251–255 (2014)
40. Knochenmuss, R.: A quantitative model of ultraviolet matrix-assisted laser desorption/ionization. J. Mass Spectrom. **37**, 867–877 (2002)
41. Gabriel, S.J., Steinhoff, R.F., Pabst, M., Schwarzinger, C., Zenobi, R., Panne, U., Weidner, S.M.: Improved analysis of ultra-high molecular mass polystyrenes in matrix-assisted laser desorption/ionization time-of-flight mass spectrometry using DCTB matrix and caesium salts. Rapid Commun. Mass Spectrom. **29**, 1039–1046 (2015)
42. Frankevich, V., Knochenmuss, R., Zenobi, R.: The origin of electrons in MALDI and their use for sympathetic cooling of negative ions in FTICR. Int. J. Mass Spectrom. **220**, 11–19 (2002)
43. Boulicault, J.E., Alves, S., Cole, R.B.: Unusual matrix for MALDI-MS of polyanionic compounds. Proceedings of the 62th Conference on Mass Spectrometry and Allied Topics, Baltimore, MD, 17 June 2014
44. Jaskolla, T.W., Karas, M.: Compelling evidence for lucky survivor and gas phase protonation: the unified MALDI analyte protonation mechanism. J. Am. Soc. Mass Spectrom. **22**, 976–988 (2011)
45. Shannon, R.D.: Revised effective ionic radii and systematic studies of interatomic distances in halides and chaleogenides. Acta Cryst **A32**, 751 (1976)
46. Deery, M.J., Jennings, K.R., Jasieczek, C.B., Haddleton, D.M., Jackson, A.T., Yates, H.T., Scrivens, J.H.: A study of cation attachment to polystyrene by means of matrix-assisted laser desorption/ionization and

electrospray ionization-mass spectrometry. Rapid Commun. Mass Spectrom. **11**, 57–62 (1997)
47. Zhang, J., Frankevich, V., Knochenmuss, R., Friess, S.D., Zenobi, R.: Reduction of Cu(II) in matrix-assisted laser desorption/ionization mass spectrometry. J. Am. Soc. Mass Spectrom. **14**, 42–50 (2003)
48. Lorion, M.M., Matt, B., Alves, S., Proust, A., Poli, G., Oble, J., Izzet, G.: Versatile post-functionalization of polyoxometalate platforms by using an unprecedented range of palladium-catalyzed coupling reactions. Chem. - A Eur. J. **19**, 12607–12612 (2013)